European Journal of Nuclear Medicine and Molecular Imaging (2024) 51:1763–1772
https://doi.org/10.1007/s00259-023-06585-7

ORIGINAL ARTICLE

Combination of [^{18}F]FDG and [^{18}F]PSMA-1007 PET/CT predicts tumour aggressiveness at staging and biochemical failure postoperatively in patients with prostate cancer

Jisu Kim[1] · Seunghwan Lee[2] · Dongwoo Kim[1] · Hyun Jeong Kim[3] · Kyeong Taek Oh[4] · Sun Jung Kim[5] · Young Deuk Choi[2] · Frederik L. Giesel[6] · Klaus Kopka[7] · Alexander Hoepping[8] · Misu Lee[9,10] · Mijin Yun[1]

Received: 21 September 2023 / Accepted: 11 December 2023 / Published online: 11 January 2024

Abstract

Purpose [^{18}F]fluorodeoxyglucose ([^{18}F]FDG) positron emission tomography/computed tomography (PET/CT) has limitations in prostate cancer (PCa) detection owing to low glycolysis in the primary tumour. Recently, prostate-specific membrane antigen (PSMA) PET/CT has been useful for biochemical failure detection and radioligand therapy (RLT) guidance. However, few studies have evaluated its use in primary prostate tumours using PSMA and [^{18}F]FDG PET/CT. This study aimed to evaluate [^{18}F]PSMA-1007 and [^{18}F]FDG PET/CT for primary tumour detection and understand the association of metabolic heterogeneity with clinicopathological characteristics at staging and postoperatively.

Method This prospective study included 42 index tumours (27 acinar and 15 ductal-dominant) in 42 patients who underwent [^{18}F]PSMA-1007 and [^{18}F]FDG PET/CT and subsequent radical prostatectomy. All patients were followed for a median of 26 mo, and serum prostate-specific antigen levels were measured every 3 mo to evaluate biochemical failure. One-way analysis of variance, Tukey's multiple comparison test, and Fisher's exact test were performed.

Results All 42 index tumours were detected on [^{18}F]PSMA-1007 PET/CT, whereas only 15 were detected on [^{18}F]FDG PET/CT (62.3% vs. 37.7%, $p < 0.0001$). A high SUV_{max} for [^{18}F]PSMA-1007 was observed in tumours with high Gleason scores (GS 6–7 vs. GS 8–10; 12.1 vs. 20.1, $p < 0.05$). Tumours with [^{18}F]FDG uptake were mostly ductal dominant (acinar-dominant 4/27; ductal-dominant; 11/15, $p < 0.001$), with lower [^{18}F]PSMA-1007 uptake than tumours without [^{18}F]FDG uptake (SUVmax 16.58 vs. 11.19, $p < 0.001$). There were 16.6% (7/42) of patients with pStage IV in whom the primary tumours were [^{18}F]FDG positive. Biochemical failure was observed in 14.8% (4/27) of patients with [^{18}F]FDG negative tumours but in 53.3% (8/15) of patients with [^{18}F]FDG positive tumours ($p = 0.013$).

Conclusions [^{18}F]PSMA-1007 PET/CT was superior to [^{18}F]FDG PET/CT in detecting primary PCa. In contrast, tumours with [^{18}F]FDG uptake are associated with larger size, a ductal-dominant type, and likely to undergo metastasis at staging and biochemical failure postoperatively.

Keywords Biochemical failure · Cancer metabolism · Cancer staging · [^{18}F]FDG · [^{18}F]PSMA-1007 PET/CT · Prostate

Introduction

Prostate cancer (PCa) is one of the most common solid tumours in men and the second leading cause of cancer-related death worldwide [1]. The diagnosis of PCa involves digital rectal examination and prostate-specific antigen (PSA) blood test, followed by transrectal ultrasound- or magnetic resonance imaging (MRI)-guided biopsy. MRI-guided biopsy can potentially improve the diagnosis and treatment [2]. This would be especially beneficial in men with prior negative biopsy results [3]. Thus, MRI has become the most favourable diagnostic modality for detecting clinically significant PCa. Unlike MRI, [^{18}F]fluorodeoxyglucose ([^{18}F]FDG) positron emission tomography/computed tomography (PET/CT) is limited in detecting PCa owing to its low glycolytic metabolism. This is attributed to the high citrate content in the prostate gland which inhibits glucose uptake by cancer cells. In contrast, PCa expresses a unique

Jisu Kim and Seunghwan Lee contributed equally to this work.

Extended author information available on the last page of the article

membrane-bound glycoprotein, prostate-specific membrane antigen (PSMA), at substantially higher levels than benign prostatic lesions [4]. PSMA combined with various radionuclides has shown great potential as a new theranostic approach for detecting PCa [5, 6].

[^{18}F]PSMA-1007, a novel PSMA-based radiopharmaceutical for PCa imaging, was developed as an alternative to [^{68}Ga]PSMA-11. The detection rates of [^{18}F]PSMA-1007 are comparable to or higher than those of [^{68}Ga]labelled PSMA ligands in patients with biochemical failure [7]. In evaluating primary prostate cancer (PCa) and regional lymph nodes (LN), [^{18}F]PSMA-1007 has an advantage due to hepatobiliary elimination. This advantage arises because no significant radioactivity is observed in the bladder, which would otherwise result in reconstruction artifacts. PCa exhibits a wide range of PSMA expression levels and uptake of PSMA-targeted radiotracers on PET/CT. PSMA uptake on PET/CT is positively correlated with the Gleason score (GS) of histopathological specimens [8]. Besides GS, the association between PSMA uptake in primary tumours and clinicopathological characteristics, such as histological subtypes, glycolytic metabolism, LN or distant metastasis, and biochemical failure after initial treatment, remains unclear.

Recent findings indicate that some patients present with high inter- or intra-lesional heterogeneity and may develop PSMA-negative tumour phenotypes [9]. In response to this challenge, a multi-tracer approach was implemented. [^{18}F]FDG PET/CT emerges as a valuable tool for detecting tumours in aggressive or castration-resistant prostate cancer (CRPC) cases with higher glucose metabolism, which may undetected in PSMA targeting imaging [10–12]. Recent studies have revealed a few more cases with either absent or low PSMA uptake but high [^{18}F]FDG activity [13, 14]. Although the combination of [^{18}F]FDG and PSMA PET/CT has been used to detect recurrent tumours in patients with biochemical failure [15], no studies have evaluated the characteristics of [^{18}F]PSMA-1007 and [^{18}F]FDG uptake on PET/CT in primary tumours at initial staging. In this study, we aimed to evaluate the role of [^{18}F]PSMA-1007 and [^{18}F]FDG PET/CT in primary tumour detection and to understand the significance of metabolic heterogeneity in relation to clinicopathological characteristics at staging and postoperatively.

Materials and methods

Study participants

This prospective, non-randomised, single-centre trial included patients with newly diagnosed, histologically confirmed intermediate- or high-risk PCa according to the D'Amico classification [16]. The inclusion criteria included men with a confirmed histological diagnosis of either intermediate (characterized by PSA levels between 10 and 20 ng/mL or a Gleason score equal to 7) or high-risk (indicated by a PSA level above 20 ng/mL or a Gleason score of 8 or higher) prostate cancer, and who were older than 18 years. The exclusion criteria included a history of any other active cancer in the past five years. Additionally, patients who had received any form of treatment for their prostate cancer disease, including but not limited to, surgery, radiotherapy, brachytherapy, or hormone therapy, were also excluded from the study. A total of 47 patients were enrolled between June 2019 and January 2021. Forty-two patients who underwent [^{18}F]PSMA-1007 and [^{18}F]FDG PET/CT during the initial staging workup and subsequent radical prostatectomy were included in the final analysis (Fig. 1a).

PET/CT scans were obtained within 1 week of each other, and radical prostatectomy was performed at a median of 7 d (interquartile range [IQR], 5–15 d) after imaging. All patients were followed for a median of 26 mo (IQR: 23–33 mo) after surgery, and serum PSA levels were measured every 3 mo. A postoperative PSA level of 0.2 ng/mL or higher, after the nadir PSA had decreased to <0.1 ng/mL, was indicative of biochemical failure. If the PSA level did not drop to <0.1 ng/mL after surgery, biochemical failure was defined as two consecutive increases from the lowest PSA value [17, 18]. This prospective study was approved by the Institutional Review Board of the Yonsei University Health System (No. 4-2018-1212), and informed consent was obtained from all patients. This study was registered with the Clinical Research Information Service (cris.nih.go.kr, KCT0004476).

PET/CT imaging protocol

For the [^{18}F]PSMA-1007 scan, approximately 250 MBq of [^{18}F]PSMA-1007 was administered intravenously 90 min before image acquisition. Images from the cerebellum to the proximal thigh were acquired using a PET/CT scanner (Discovery 710; General Electric Medical Systems, Milwaukee, WI, USA) with low-dose CT transmission (60 mA, 120 kVp). PET emission scans were performed for 2.5 min per bed in a three-dimensional mode. For [^{18}F]FDG PET/CT, all patients were asked to fast for at least 6 h before radiotracer injection to ensure that their blood glucose levels did not exceed 140 mg/dL. Approximately 5.5 MBq of [^{18}F]FDG per kg of body weight was administered intravenously 1 h before image acquisition. Images from the cerebellum to the proximal thigh were acquired using a PET-CT scanner (Biograph TruePoint 40; Siemens Healthcare, Erlangen, Germany) with low-dose CT transmission (auto mA, 120 kVp). PET emission scans were performed for 2.5 min per

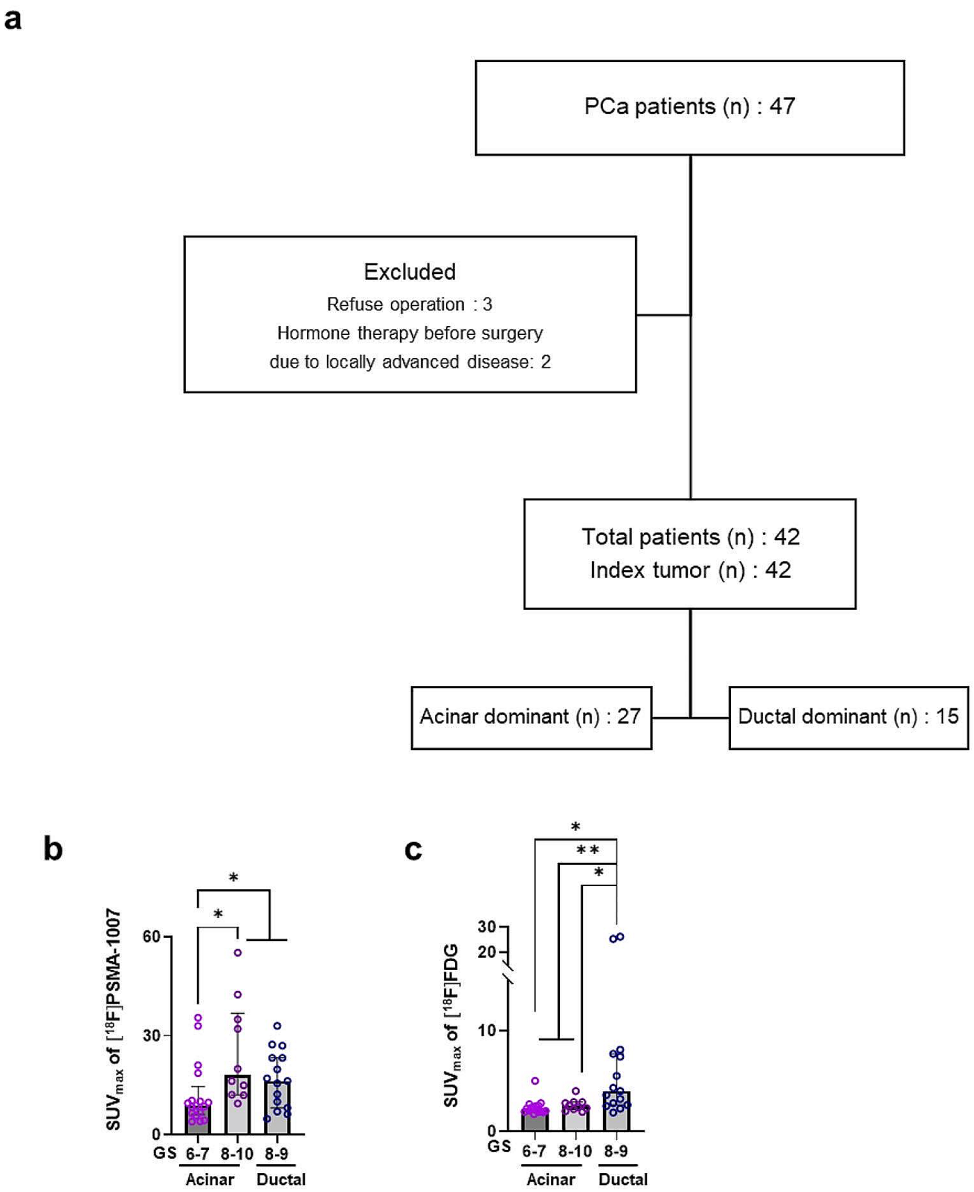

Fig. 1 Maximum standardised uptake value (SUV_{max}) of [^{18}F]prostate-specific membrane antigen (PSMA)-1007 and [^{18}F]fluorodeoxyglucose (FDG) according to the Gleason score (GS) and histological subtype. (**a**) Patient flow chart. (**b, c**) SUV_{max} of [^{18}F]PSMA-1007 (**b**) and [^{18}F]FDG (**c**) is evaluated according to GS and histological subtypes (19 tumours with GS 6−7 are acinar-dominant, 8 with GS 8–9 are acinar-dominant, and 15 with GS 8–9 are ductal-dominant subtypes). Data are presented as median and statistically analysed. *$p < 0.05$, **$p < 0.01$

bed in three-dimensional mode. PET images were iteratively reconstructed using attenuation, scatter, and random corrections.

Dice similarity coefficient (DICE) score

We delineated the Regions of Interest (ROI) for prostate cancer in ADC MRI and compared these with [^{18}F]PSMA-1007 and [^{18}F]FDG PET ROIs to calculate the DICE score following previous method [19]. ROIs were manually segmented by a nuclear medicine physician. The DICE score computation was carried out using Matlab (MathWorks, Massachusetts, USA) while all statistical analyses were performed in GraphPad Prism version 8.

Image analysis

[^{18}F]PSMA-1007 and [^{18}F]FDG PET/CT images were registered as diffusion-weighted images, apparent diffusion coefficient maps, and T2-weighted images of the prostate on MRI using the MIM imaging software (MIM-6.5; MIM Software Inc., Cleveland, OH, USA). Intraprostatic findings were validated using MRI and histological data from apex to base of prostate. Two board-certified nuclear medicine physicians with 27 and 7 year of PET/CT experience analysed [^{18}F]-PSMA-1007 and [^{18}F]FDG uptake in each index tumour using visual and semi-quantitative analyses. SUV was calculated as follows: [decay-corrected activity (kBq) per tissue volume (mL)]/[injected [^{18}F-FDG] activity (kBq) per body mass (g)]. A volume of interest was drawn over

the site of the most intense [^{18}F]PSMA-1007 uptake in the tumour lesion on transaxial images, and the maximum SUV (SUV_{max}) of the tumour was measured.

The index tumour was deemed positive for [^{18}F]PSMA-1007 if it exhibited elevated uptake of [^{18}F]PSMA-1007 compared to the surrounding normal prostate gland, and positive for [^{18}F]FDG if it demonstrated increased uptake of [^{18}F]FDG relative to the surrounding normal prostate gland. Follow-up imaging was performed to confirm the presence of metastatic lesions that could not be confirmed histopathologically. A decrease in lesion volume combined with a decrease in PSA levels during therapy was considered a sign of malignancy. Moreover, lesions with increasing volumes and PSA levels were considered malignant.

Histological evaluation

Whole-mount histological slices were cut from the prostatectomy specimens. Haematoxylin-eosin-stained whole-mount pathology slides were obtained, and a pathologist delineated the index tumours. The index tumours were categorized into acinar or ductal types according to the dominant histology of the tumour, with largest tumours being of one type or the other, and then classified as low-GS (GS 6 and 7) or high-GS (GS 8–10) [20]. Finally, the tumours were classified into the following three groups according to the histological subtype and GS: low-GS acinar-dominant, high-GS acinar-dominant, and high-GS ductal-dominant.

Statistical analysis

Statistical analyses were performed using the GraphPad Prism software (GraphPad Software Inc.). Pearson's correlation coefficient was calculated to measure the correlation between SUV_{max} and tumour volume and SUV_{max}. One-way analysis of variance was used to compare the SUV_{max} levels of index tumours, and Tukey's multiple comparison test was used to control for multiple comparisons in the post-hoc analyses. PSMA uptake in [^{18}F]FDG-positive and [^{18}F]FDG-negative regions was analysed using the paired t-test. The Fisher's exact test was used to compare the frequency of metastatic tumours and biochemical failure between [^{18}F]FDG-positive and [^{18}F]FDG-negative PCa. The results were expressed as the means ± standard error of the mean (range). Statistical significance was set at $p < 0.05$.

Results

Characteristics of the patients

This study included 42 patients with a median age of 70 year (range: 57–85 year). All patients underwent radical prostatectomy. The majority had robot-assisted radical prostatectomy (38 patients), while retropubic radical prostatectomy was performed in 4 patients. Postoperative hormone therapy was administered to 10 patients, with 7 receiving leuprolide and 3 receiving goserelin. Four patients received postoperative radiotherapy. Additionally, one patient received concurrent postoperative hormone therapy (goserelin) with. Among patients experiencing biochemical failure, the mean PSA doubling time was 5.1 months, with a range of 2.0 to 9.6 months. The PSA values ranged from 3.02 to 265.1 ng/mL (median, 11 ng/mL). A total of 17, 16, and 9 patients had disease of clinical stages (cStage) II, III, and IV, respectively. Six patients with cN1 underwent pelvic LN dissection, and five had pathological stage (pStage) N1 disease. In the remaining patient, no LN metastasis was observed on pathological examination. However, the patient was classified as having pN1 disease because of persistent PSA elevation after surgery and subsequent reduction in LN volume and PSA levels after androgen-deprivation therapy. Of the three patients with cM1 (bone metastasis), one was confirmed to have metastases; however, no tumour was observed in the remaining two patients upon bone biopsy. One of the two patients demonstrated elevated PSA levels after surgery and received radiotherapy for the bone lesion, resulting in decreased PSA levels; hence, it was classified as pM1. The other patient attained a PSA level of < 0.1 ng/mL after surgery, and his disease was classified as pM0.

Among the index tumours, 64.3% (27/42) were of acinar-dominant and 35.7% (15/42) were of ductal-dominant (Table 1) subtypes. Among the acinar-dominant tumours, 4, 15, 2, and 6 patients exhibited GSs of 6, 7, 8, 9, and 10, respectively. Among the ductal-dominant tumours, 12 and 3 had GSs of 8 and 9, respectively (Table 2). The detailed patient characteristics are summarised in Tables 1 and 2.

SUV_{max} of [^{18}F]PSMA-1007 and [^{18}F]FDG according to histological subtypes and GS

When tumours were categorised according to the histological subtype and GS, the SUV_{max} of [^{18}F]PSMA-1007 was higher in high-GS acinar- and ductal-dominant tumours than that in low-GS acinar-dominant tumours (SUV_{max} 12.1, low-GS acinar vs. 20.1, high-GS acinar and ductal, $p < 0.05$, Fig. 1b). In contrast, the SUV_{max} of [^{18}F]FDG was higher in the ductal-dominant than in the acinar-dominant tumours (SUV_{max} 2.5, acinar vs. 7.2, ductal, $p < 0.05$, Fig. 1c).

Table 1 Clinicopathological characteristics of the patients

Patients (n)		42	
Age (years)			
Median (range)		70 (50–85)	
PSA (ng/mL)			
Median (range)		11 ng/mL (3.02–265.1)	
Clinical stage		n	%
II	IIA	3	7%
	IIB	2	5%
	IIC	12	29%
III	IIIA	3	7%
	IIIB	7	17%
	IIIC	6	14%
IV	IVA	4	10%
	IVB	5	11%
Pathologic stage		N	%
II	IIA	1	2%
	IIB	3	7%
	IIC	7	17%
III	IIIA	1	2%
	IIIB	16	38%
	IIIC	7	16%
IV	IVA	5	12%
	IVB	2	6%
Risk according to D 'Amico classification		n	%
Intermediate		9	21%
High		33	79%
Tumour size (cc)			
Median (range)		2.2 (0.2–20)	

Table 2 Gleason score of index tumours

		Adenocarcinoma			
		Acinar dominant		Ductal dominant	
		N	%	*N*	%
Index tumours (n)	42	27	64%	15	36%
Gleason score (n of index tumor)					
6	4	4	100%	0	0%
7a	6	6	100%	0	0%
7b	9	9	100%	0	0%
8	14	2	14%	12	86%
9–10	9	6	67%	3	33%

Metabolic patterns between [^{18}F]PSMA-1007 and [^{18}F]FDG uptake in index tumours

All 42 index tumours were detected on [^{18}F]PSMA-1007 PET/CT, whereas only 15 (35.7%) were detected on [^{18}F]FDG PET/CT. Among the histological subtypes, tumours with [^{18}F]FDG uptake were mostly of ductal-dominant subtypes (73%, 11/15) and had significantly larger tumour volumes than those without [^{18}F]FDG uptake on pathology (mean tumour volume, 6.06 cc vs. 2.54 cc, $p = 0.017$). Also, tumours without [^{18}F]FDG uptake predominantly exhibited a lower GS (GS 6–7: 66.8%, GS 8–9: 33.2%). whereas tumours with [^{18}F]FDG uptake demonstrated a higher GS (GS 6–7: 6.7%, GS 8–9: 93.3%). In the [^{18}F]FDG-positive tumours, we observed a reciprocal pattern of metabolism between [^{18}F]PSMA-1007 and [^{18}F]FDG uptake; areas with increased [^{18}F]FDG uptake demonstrated low [^{18}F]PSMA-1007 uptake and vice versa (Fig. 2a). Semi-quantitatively, tumour regions with [^{18}F]FDG uptake demonstrated a significantly lower SUV_{max} of [^{18}F]PSMA-1007 than tumour regions without [^{18}F]FDG uptake (11.19 vs. 16.58, $p < 0.001$, Fig. 2b).

Dice similarity coefficient (DICE) score

For [^{18}F]FDG-negative tumours, we observed a high mean DICE score of 0.82 (range: 0.69–0.90) between MRI and [^{18}F]PSMA ROIs in [^{18}F]FDG-negative tumours. In [^{18}F]FDG-positive tumours, there was a relatively lower mean DICE score (PSMA: 0.70, range: 0.59–0.77; FDG: 0.46, range: 0.22–0.64) attributable to the disparate areas of high [^{18}F]PSMA and [^{18}F]FDG uptake observed in the MRI ROIs (Supplementary Fig. 1).

Clinical significance of tumours with [^{18}F]FDG uptake at staging and postoperatively

Among the 42 patients, 7 exhibited pStage IV disease (pN1M0 (n = 5), pN0M1 (n = 1), and pN1M1 (n = 1). All patients with [^{18}F]FDG positive primary tumours, whereas no patients with [^{18}F]FDG negative tumour exhibited pStage IV ($p < 0.0001$, Fig. 3a and c). The preoperative PSA levels were higher in patients with [^{18}F]FDG positive primary tumours compared to those with [^{18}F]FDG negative tumours (63.92 ng/ml vs. 14.21 ng/ml, p value = 0.008). After surgery, biochemical failure was observed in 14.8% (4/27) of patients with [^{18}F]FDG negative tumours and 53.3% (8/15) of patients with [^{18}F]FDG positive tumours ($p = 0.0132$, Fig. 3d). In summary, tumours with [^{18}F]FDG uptake were associated with metastatic disease at staging and biochemical failure after surgery.

Discussion

PET/CT, combined with radiotracers that target specific molecules of clinical significance, is a promising imaging modality for cancer diagnosis and therapy. [^{18}F]PSMA has emerged as the radiotracer of choice for detecting recurrent PCa [21–23]. In the present study, we observed that [^{18}F]PSMA-1007 PET/CT was significantly more useful than [^{18}F]FDG PET/CT in detecting index tumours of the prostate gland (100% vs. 35.7%) at initial staging. In

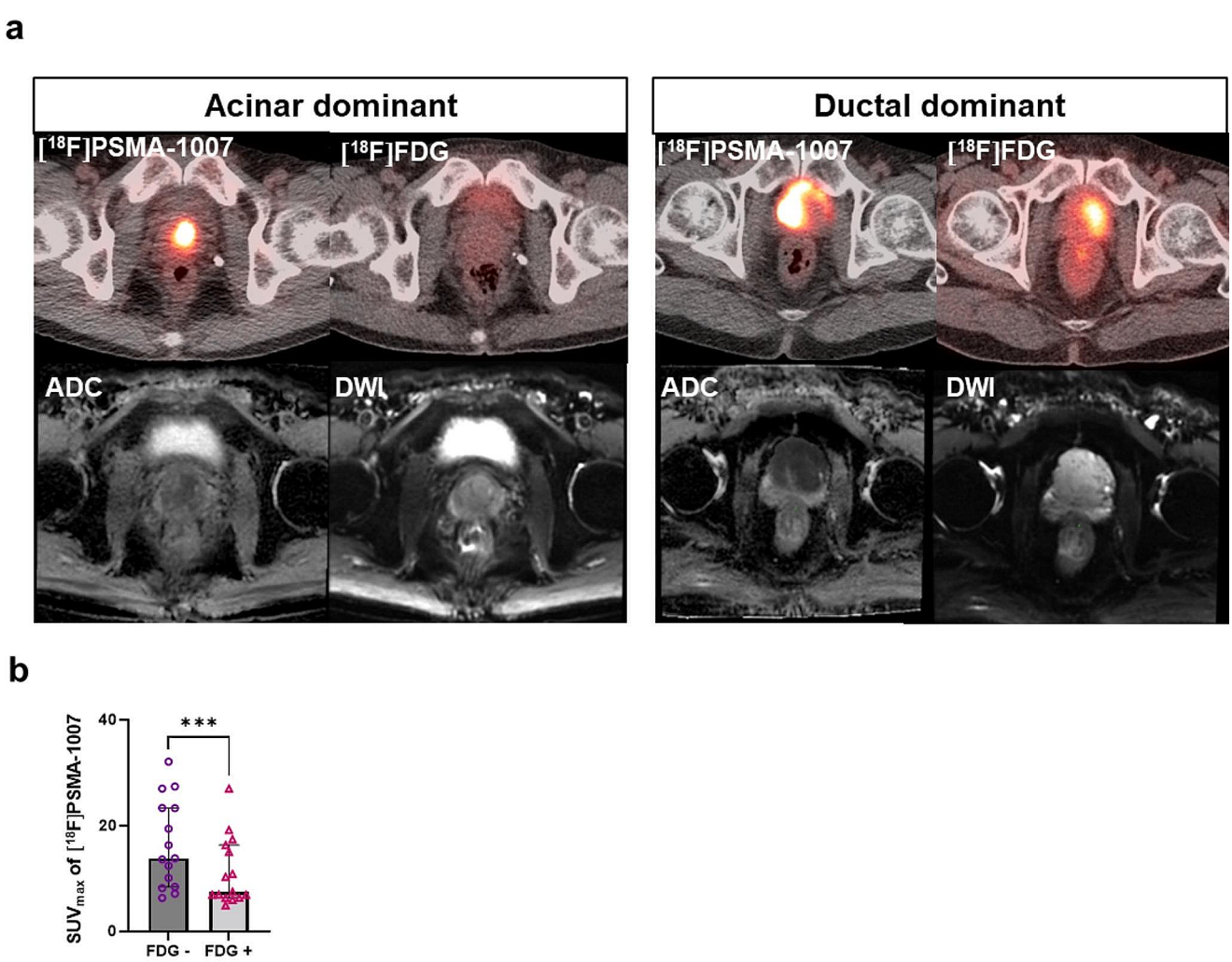

Fig. 2 Correlation of the maximum standardised uptake value (SUV_{max}) of [^{18}F]prostate-specific membrane antigen (PSMA)-1007 and [^{18}F]fluorodeoxyglucose (FDG) in index tumours. (**a**) Maximum intensity projection and axial images of [^{18}F]PSMA-1007 and [^{18}F]FDG positron emission tomography/computed tomography in acinar- and ductal-dominant prostate cancer. ADC; apparent diffusion coefficient, DWI; diffusion-weighted image (**b**) The SUV_{max} of [^{18}F]PSMA-1007 is compared between the tumour regions with and without [^{18}F]FDG uptake in patients with [^{18}F]FDG-positive tumour. Data are presented as median and statistically analysed using an unpaired two-tailed t-test. ***$p < 0.001$

contrast, tumours with [^{18}F]FDG uptake were large, of mostly ductal-dominant type, and likely to undergo metastasis at staging and biochemical failure after surgery. Interestingly, tumour regions with [^{18}F]FDG uptake demonstrated a significantly lower SUVmax of [^{18}F]PSMA-1007 than that of tumour regions without [^{18}F]FDG uptake.

Although [^{11}C]Choline and [^{18}F]Fluciclovine have been used clinically to identify PCa, their specificity is limited. [^{68}Ga]PSMA exhibited higher diagnostic accuracy for PCa than that of [^{11}C]Choline [24] and significantly higher tracer uptake in tumours with a GS of 7–10 than in those with a GS of 6 or lower [25]. In addition, the use of a multitracer approach, in combination with other tracers such as [^{68}Ga]Ga-DOTA-RM2 PET/MRI, demonstrated better prediction of high-risk prostate cancer staging [26]. However, [^{68}Ga]labelled compounds have limitations related to their short half-life, large position range that affects image quality, and relatively low availability. Recently, [^{18}F]labelled PSMA ligands demonstrated higher detection rates of recurrent tumours within the prostate bed and surrounding pelvic structures following prostatectomy than those of [^{68}Ga]labelled ligands [27]. [^{18}F]PSMA-1007 uptake also correlated with GS, with low uptake in low-grade tumours (GS 6 and 7a) and high uptake in high-grade tumours (GS 8 and 9) [28]. In this study, we compared [^{18}F]PSMA uptake among different GS and histological subtypes. [^{18}F]PSMA-1007 uptake on PET/CT demonstrated a strong correlated with GS. However, the degree of [^{18}F]PSMA-1007 uptake was not useful for differentiating between the acinar and ductal histologies.

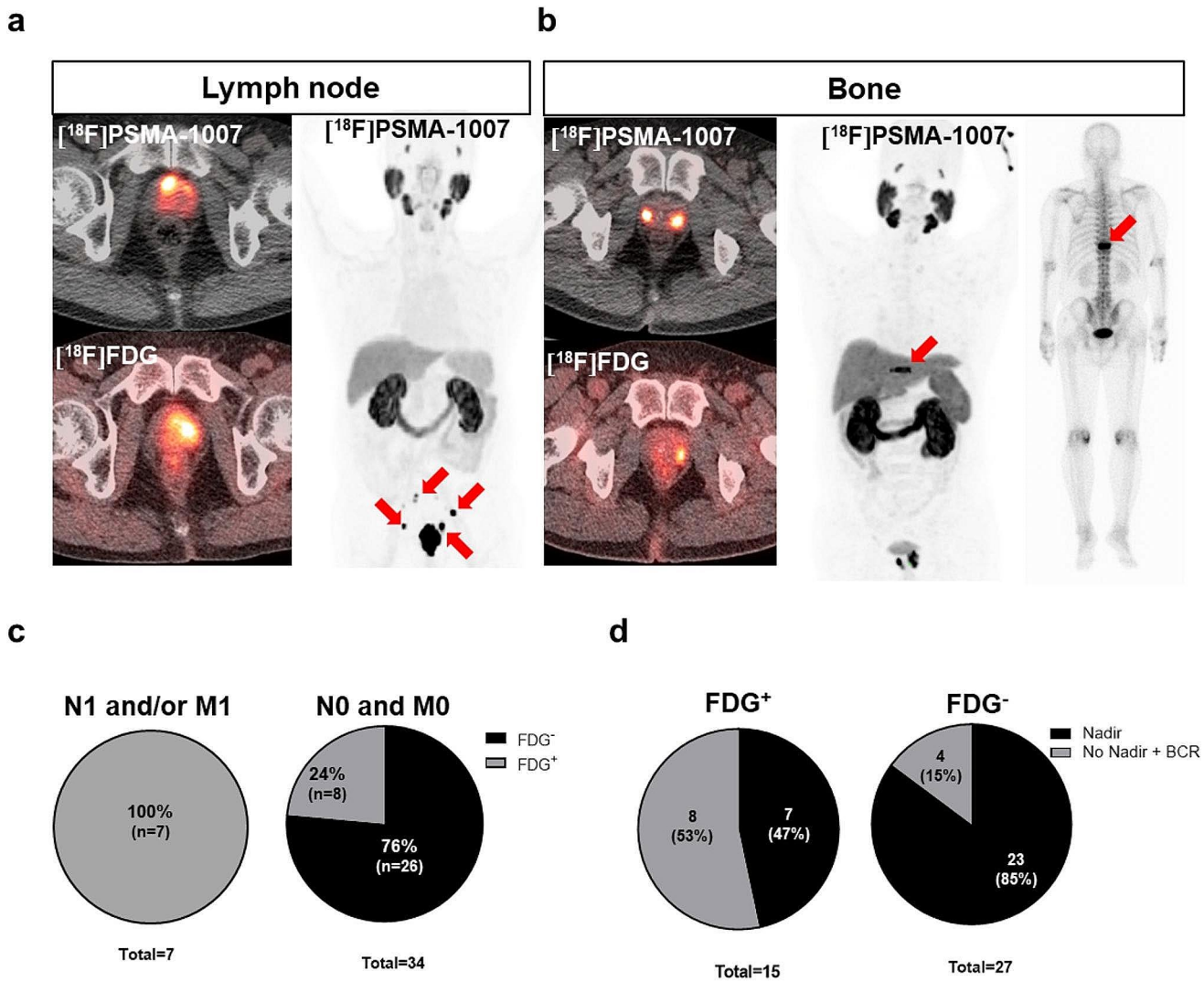

Fig. 3 Clinical significance of tumours with [^{18}F]fluorodeoxyglucose (FDG) uptake. (**a**) A patient with lymph node metastasis: left axial images of [^{18}F]PSMA-1007 and [^{18}F]FDG positron emission tomography/computed tomography. Maximum intensity projection (MIP) image of [^{18}F]PSMA-1007 revealing lymph node metastases (red arrows). (**b**) A patient with bone metastasis: left axial images of [^{18}F]PSMA-1007 and [^{18}F]FDG positron emission tomography/computed tomography. MIP image of [^{18}F]PSMA-1007 revealing lymph node metastases (red arrows). A posterior view of planar bone scan revealing a bone metastasis (right, red arrow). (**c**) The frequency of lymph node (N) or distant (M) metastases is compared between [^{18}F]FDG-positive (n = 15) and negative prostate cancer (PCa) (n = 27). (**d**) The frequency of biochemical failure is compared between [^{18}F]FDG-positive (n = 15) and negative PCa (n = 27)

Unlike [^{18}F]PSMA-1007, we observed interesting clinicopathological characteristics related to [^{18}F]FDG uptake in primary tumours. First, [^{18}F]FDG uptake on PET/CT closely correlated with ductal-dominant histology. The ductal type is a rare aggressive variant of PCa with poor prognosis and limited therapeutic options than the acinar type [29]. In this study, 15 of the 42 index tumours exhibited a ductal-dominant histology, which appeared to be highly prevalent probably because of the detailed classification of the proportion of histological subtypes in the index tumours. Second, tumours with [^{18}F]FDG uptake were significantly larger, had higher GS, and initial PSA concentrations than those without [^{18}F]FDG uptake. Che et al. also demonstrated that [^{68}Ga]PSMA-negative tumour lesions with [^{18}F]FDG-positive in patients with castration-resistant PCa showed higher PSA and GS levels than those without [30]. Most importantly, tumours with [^{18}F]FDG uptake exhibited higher LN and/or distant metastasis at staging and higher postoperative biochemical failure rates than those of tumours without [^{18}F]FDG uptake. Our study suggested that the addition of [^{18}F]FDG PET/CT to [^{18}F]PSMA PET/CT can help identify tumours with aggressive biology. These results are consistent with those of previous reports demonstrating high [^{18}F]FDG uptake in primary tumours with

a GS > 7 [31] and in tumours with biologically aggressive characteristics [32].

Tumours with positive [^{18}F]FDG uptake may have important therapeutic implications. In a recent prospective trial of [^{68}Ga]PSMA and [^{18}F]FDG PET/CT, which included 37 patients with early PSA progression during castration, 29% (33/114) of the lesions demonstrated negative [^{68}Ga]PSMA but positive [^{18}F]FDG uptake, and this was observed more frequently in the castration-resistant cohort than in the hormone-sensitive cohort [33]. Although randomised controlled trials have shown the efficacy of lutetium-177 [^{177}Lu]PSMA-based radioligand therapy (RLT) for patients with metastatic castration-resistant PCa [34], tumours with positive [^{18}F]FDG uptake are negative predictors of overall survival [35]. In our study, we identified primary tumours with positive [^{18}F]FDG uptake at initial staging. These tumours exhibited a tendency to undergo metastasis with ductal-dominant histology and display low [^{18}F]PSMA-1007 uptake which could hold significant implications in predicting poor responses to RLT and hormone suppression therapy.

One limitation of this study was that the proportion of patients with stage IV disease (7/42, 16.7%) was low. Consequently, the diagnostic performance of [^{18}F]PSMA PET/CT for LN or distant metastases could not be evaluated in detail. This study only correlated the imaging and pathological findings of the index tumours. For secondary lesions of the prostate gland, collaborative efforts among pathologists, radiologists, and nuclear medicine physicians are essential. Detailed histopathological evaluation of the entire prostate gland is required to thoroughly evaluate each lesion. In future studies, we plan to perform imaging and pathological analyses of secondary tumours of the prostate gland. The other limitation of our study is that different PET scanners were used for [^{18}F]PSMA-1007 and [^{18}F]FDG scans. Specifically, all [^{18}F]PSMA-1007 scans were performed using one PET scanner, while [^{18}F]FDG scans were carried out on another PET scanner. This consistent application of dedicated scanners for each type of radiotracer ensured accurate and uniform visual and SUV analyses within each tracer group, ensuring that the results were not influenced by differences between scanners.

[^{18}F]PSMA-1007 PET/CT is superior to [^{18}F]FDG PET/CT in detecting primary PCa. Compared with the [^{18}F]FDG-negative tumours and [^{18}F]FDG-positive tumours are larger, of mostly ductal-dominant type, and are more likely to undergo metastasis at staging and biochemical failure after surgery.

Supplementary Information The online version contains supplementary material available at https://doi.org/10.1007/s00259-023-06585-7.

Acknowledgements N/A.

Author contributions All authors contributed to the study conception and design. Material preparation, data collection, and analysis were performed by Jisu Kim, Seunghwan Lee, Misu Lee, and Mijin Yun. The first draft of the manuscript was written by Jisu Kim, Seunghwan Lee, Misu Lee, and Mijin Yun and all authors commented on previous versions of the manuscript. All authors read and approved the final manuscript.

Funding This research was supported by the National Research Foundation of Korea (grant numbers NRF-2016K1A3A1A48953207, NRF-2020R1A2B5B01098109, and RS-2022-00144475).

Data availability The datasets generated during and/or analysed during the current study are available from the corresponding author on reasonable request.

Declarations

Ethics statement The Institutional Review Board of our hospital approved the study, and informed consent was obtained from all the patients.

Competing interests The authors have no relevant financial or non-financial interests to disclose.

References

1. Rawla P. Epidemiology of Prostate Cancer. World J Oncol. 2019;10:63–89. https://doi.org/10.14740/wjon1191
2. Drost FH, Osses DF, Nieboer D, Steyerberg EW, Bangma CH, Roobol MJ, et al. Prostate MRI, with or without MRI-targeted biopsy, and systematic biopsy for detecting Prostate cancer. Cochrane Database Syst Rev. 2019;4:CD012663. https://doi.org/10.1002/14651858.CD012663.pub2
3. Woodrum DA, Gorny KR, Greenwood B, Mynderse LA. MRI-Guided prostate biopsy of native and recurrent Prostate Cancer. Semin Interv Radiol. 2016;33:196–205. https://doi.org/10.1055/s-0036-1586151
4. Troyer JK, Beckett ML, Wright GL. Jr. Detection and characterization of the prostate-specific membrane antigen (PSMA) in tissue extracts and body fluids. Int J Cancer. 1995;62:552–8. https://doi.org/10.1002/ijc.2910620511
5. Oh SW, Suh M, Cheon GJ. Current status of PSMA-Targeted Radioligand Therapy in the era of Radiopharmaceutical Therapy acquiring marketing authorization. Nucl Med Mol Imaging. 2022;56:263–81.
6. Al-Ibraheem A, Scott AM. (161)Tb-PSMA unleashed: a Promising New Player in the theranostics of Prostate Cancer. Nucl Med Mol Imaging. 2023;57:168–71.
7. Giesel FL, Knorr K, Spohn F, Will L, Maurer T, Flechsig P, et al. Detection efficacy of (18)F-PSMA-1007 PET/CT in 251 patients with biochemical recurrence of Prostate Cancer after Radical Prostatectomy. J Nucl Med. 2019;60:362–8. https://doi.org/10.2967/jnumed.118.212233
8. Lisney AR, Leitsmann C, Strauss A, Meller B, Bucerius JA, Sahlmann CO. The role of PSMA PET/CT in the primary diagnosis and Follow-Up of prostate Cancer-A practical clinical review. Cancers. 2022;14. doi:ARTN 363810.3390/cancers14153638.
9. Paschalis A, Sheehan B, Riisnaes R, Rodrigues DN, Gurel B, Bertan C, et al. Prostate-specific membrane Antigen

Heterogeneity and DNA repair defects in Prostate Cancer. Eur Urol. 2019;76:469–78.
10. Lavallee E, Bergeron M, Buteau FA, Blouin AC, Duchesnay N, Dujardin T, et al. Increased Prostate Cancer glucose metabolism detected by (18)F-fluorodeoxyglucose Positron Emission Tomography/Computed Tomography in Localised Gleason 8–10 prostate cancers identifies very high-risk patients for early recurrence and resistance to Castration. Eur Urol Focus. 2019;5:998–1006. https://doi.org/10.1016/j.euf.2018.03.008
11. Wang B, Liu C, Wei Y, Meng J, Zhang Y, Gan H, et al. A prospective trial of (68)Ga-PSMA and (18)F-FDG PET/CT in nonmetastatic Prostate Cancer patients with an early PSA Progression during Castration. Clin Cancer Res. 2020;26:4551–8. https://doi.org/10.1158/1078-0432.CCR-20-0587
12. Shen K, Liu B, Zhou X, Ji Y, Chen L, Wang Q, et al. The evolving role of (18)F-FDG PET/CT in diagnosis and prognosis prediction in Progressive Prostate Cancer. Front Oncol. 2021;11:683793. https://doi.org/10.3389/fonc.2021.683793
13. Hofman MS, Violet J, Hicks RJ, Ferdinandus J, Thang SP, Akhurst T, et al. [(177)Lu]-PSMA-617 radionuclide treatment in patients with metastatic castration-resistant Prostate cancer (LuPSMA trial): a single-centre, single-arm, phase 2 study. Lancet Oncol. 2018;19:825–33. https://doi.org/10.1016/S1470-2045(18)30198-0
14. Alberts I, Schepers R, Zeimpekis K, Sari H, Rominger A, Afshar-Oromieh A. Combined [68 Ga]Ga-PSMA-11 and low-dose 2-[18F]FDG PET/CT using a long-axial field of view scanner for patients referred for [177Lu]-PSMA-radioligand therapy. Eur J Nucl Med Mol Imaging. 2023;50:951–6. https://doi.org/10.1007/s00259-022-05961-z
15. Chen RH, Wang YN, Zhu YJ, Shi YP, Xu L, Huang G, et al. The added value of F-18-FDG PET/CT compared with Ga-68-PSMA PET/CT in patients with castration-resistant Prostate Cancer. J Nucl Med. 2022;63:69–75. https://doi.org/10.2967/jnumed.120.262250
16. Cantiello F, Gangemi V, Cascini GL, Calabria F, Moschini M, Ferro M, et al. Diagnostic accuracy of (64)copper prostate-specific membrane Antigen Positron Emission Tomography/Computed tomography for primary lymph node staging of Intermediate-to high-risk Prostate Cancer: our preliminary experience. Urology. 2017;106:139–45. https://doi.org/10.1016/j.urology.2017.04.019
17. Heo JE, Park JS, Lee JS, Kim J, Jang WS, Cho NH, et al. Postoperative biochemical recurrence of pathologically localized high-grade Prostate cancer in adjuvant treatment-naive patients. J Cancer Res Clin Oncol. 2020;146:221–7. https://doi.org/10.1007/s00432-019-03049-0
18. Kang YJ, Kim HS, Jang WS, Kwon JK, Yoon CY, Lee JY, et al. Impact of lymphovascular invasion on lymph node Metastasis for patients undergoing radical prostatectomy with negative resection margin. BMC Cancer. 2017;17:321. https://doi.org/10.1186/s12885-017-3307-4
19. Ghezzo S, Neri I, Mapelli P, Savi A, Samanes Gajate AM, Brembilla G, et al. [(68)Ga]Ga-PSMA and [(68)Ga]Ga-RM2 PET/MRI vs. histopathological images in Prostate Cancer: a New Workflow for spatial Co-registration. Bioeng (Basel). 2023;10. https://doi.org/10.3390/bioengineering10080953
20. Huang CC, Deng FM, Kong MX, Ren Q, Melamed J, Zhou M. Re-evaluating the concept of dominant/index Tumor nodule in multifocal Prostate cancer. Virchows Arch. 2014;464:589–94. https://doi.org/10.1007/s00428-014-1557-y
21. Olivier P, Giraudet AL, Skanjeti A, Merlin C, Weinmann P, Rudolph I, et al. Phase III study of (18)F-PSMA-1007 Versus (18)F-Fluorocholine PET/CT for localization of Prostate Cancer biochemical recurrence: a prospective, randomized, crossover Multicenter Study. J Nucl Med. 2023;64:579–85.
22. Sprute K, Kramer V, Koerber SA, Meneses M, Fernandez R, Soza-Ried C, et al. Diagnostic accuracy of (18)F-PSMA-1007 PET/CT Imaging for Lymph Node Staging of Prostate Carcinoma in primary and biochemical recurrence. J Nucl Med. 2021;62:208–13.
23. Giesel FL, Hadaschik B, Cardinale J, Radtke J, Vinsensia M, Lehnert W, et al. F-18 labelled PSMA-1007: biodistribution, radiation dosimetry and histopathological validation of Tumor lesions in Prostate cancer patients. Eur J Nucl Med Mol Imaging. 2017;44:678–88.
24. Hegemann NSS, Rogowski P, Eze C, Schafer C, Stief C, Lang S, et al. Outcome after 68Ga-PSMA-11 versus Choline PET-Based salvage radiotherapy in patients with biochemical recurrence of Prostate Cancer: a matched-pair analysis. Cancers. 2020;12. ARTN 339510.3390/cancers12113395.
25. Grubmuller B, Baltzer P, Hartenbach S, D'Andrea D, Helbich TH, Haug AR, et al. PSMA Ligand PET/MRI for primary Prostate Cancer: staging performance and clinical impact. Clin Cancer Res. 2018;24:6300–7. https://doi.org/10.1158/1078-0432.Ccr-18-0768
26. Mapelli P, Ghezzo S, Samanes Gajate AM, Preza E, Brembilla G, Cucchiara V, et al. Preliminary results of an ongoing prospective clinical trial on the Use of (68)Ga-PSMA and (68)Ga-DOTA-RM2 PET/MRI in staging of high-risk Prostate Cancer patients. Diagnostics (Basel). 2021;11. https://doi.org/10.3390/diagnostics11112068
27. Giesel FL, Knorr K, Spohn F, Will L, Maurer T, Flechsig P, et al. Detection efficacy of F-18-PSMA-1007 PET/CT in 251 patients with biochemical recurrence of Prostate Cancer after Radical Prostatectomy. J Nucl Med. 2019;60:362–8. https://doi.org/10.2967/jnumed.118.212233
28. Hong JJ, Liu BL, Wang ZQ, Tang K, Ji XW, Yin WW et al. The value of F-18-PSMA-1007 PET/CT in identifying non-metastatic high-risk prostate cancer. Ejnmmi Research. 2020;10. doi:ARTN 13810.1186/s13550-020-00730-1.
29. Montironi R, Cimadamore A, Lopez-Beltran A, Scarpelli M, Aurilio G, Santoni M et al. Morphologic, molecular and clinical features of aggressive variant Prostate Cancer. Cells. 2020;9. doi:ARTN 107310.3390/cells9051073.
30. Chen R, Wang Y, Zhu Y, Shi Y, Xu L, Huang G, et al. The added value of (18)F-FDG PET/CT compared with (68)Ga-PSMA PET/CT in patients with castration-resistant Prostate Cancer. J Nucl Med. 2022;63:69–75. https://doi.org/10.2967/jnumed.120.262250
31. Beauregard JM, Blouin AC, Fradet V, Caron A, Fradet Y, Lemay C et al. FDG-PET/CT for pre-operative staging and prognostic stratification of patients with high-grade prostate cancer at biopsy. Cancer Imaging. 2015;15. doi:ARTN 210.1186/s40644-015-0038-0.
32. Shen K, Liu B, Zhou X, Ji YY, Chen L, Wang Q et al. The Evolving Role of F-18-FDG PET/CT in Diagnosis and Prognosis Prediction in Progressive Prostate Cancer. Front Oncol. 2021;11. doi:ARTN 68379310.3389/fonc.2021.683793.
33. Wang BH, Liu C, Wei Y, Meng J, Zhang YJ, Gan HL, et al. A prospective trial of Ga-68-PSMA and F-18-FDG PET/CT in non-metastatic Prostate Cancer patients with an early PSA Progression during Castration. Clin Cancer Res. 2020;26:4551–8. https://doi.org/10.1158/1078-0432.Ccr-20-0587
34. Sadaghiani MS, Sheikhbahaei S, Werner RA, Pienta KJ, Pomper MG, Gorin MA, et al. Lu-177-PSMA radioligand therapy effectiveness in metastatic castration-resistant Prostate cancer: an updated systematic review and meta-analysis. Prostate. 2022;82:826–35. https://doi.org/10.1002/pros.24325
35. Michalski K, Ruf J, Goetz C, Seitz AK, Buck AK, Lapa C, et al. Prognostic implications of dual tracer PET/CT: PSMA ligand and [F-18]FDG PET/CT in patients undergoing [Lu-177]PSMA

radioligand therapy. Eur J Nucl Med Mol Imaging. 2021;48:2024–30. https://doi.org/10.1007/s00259-020-05160-8

Authors and Affiliations

Jisu Kim[1] · Seunghwan Lee[2] · Dongwoo Kim[1] · Hyun Jeong Kim[3] · Kyeong Taek Oh[4] · Sun Jung Kim[5] · Young Deuk Choi[2] · Frederik L. Giesel[6] · Klaus Kopka[7] · Alexander Hoepping[8] · Misu Lee[9,10] · Mijin Yun[1]

✉ Misu Lee
misulee@inu.ac.kr

✉ Mijin Yun
YUNMIJIN@yuhs.ac

[1] Department of Nuclear Medicine, Severance Hospital, Yonsei University College of Medicine, Seoul 03722, South Korea

[2] Department of Urology, Severance Hospital, Yonsei University College of Medicine, Seoul, South Korea

[3] Department of Nuclear medicine, Yongin Severance Hospital, Yonsei University College of Medicine, Yongin, South Korea

[4] Department of Medical Engineering, Yonsei University College of Medicine, Seoul, South Korea

[5] Department of Nuclear Medicine, National Health Insurance Service Ilsan Hospital, Goyang, South Korea

[6] Department of Nuclear Medicine, Medical Faculty, Heinrich-Heine-University, University Hospital Duesseldorf, Duesseldorf, Germany

[7] Institute of Radiopharmaceutical Cancer Research, Helmholtz-Zentrum Dresden-Rossendorf (HZDR), 01328 Dresden, Germany

[8] ABX Advanced Biochemical Compounds GmbH, Heinrich-Glaeser-Strasse 10-14, 01454 Radeberg, Germany

[9] Division of Life Sciences, College of Life Science and Bioengineering, Incheon National University, Incheon, South Korea

[10] Institute for New Drug Development, College of Life Science and Bioengineering, Incheon National University, Incheon 22012, South Korea